

# Metal coated polymer and paper-based cantilever design and analysis for acoustic pressure sensing

Cite as: AIP Advances **10**, 055112 (2020); <https://doi.org/10.1063/5.0006544>

Submitted: 05 March 2020 • Accepted: 18 April 2020 • Published Online: 12 May 2020

 R. B. Mishra,  S. F. Shaikh,  A. M. Hussain, et al.



View Online



Export Citation



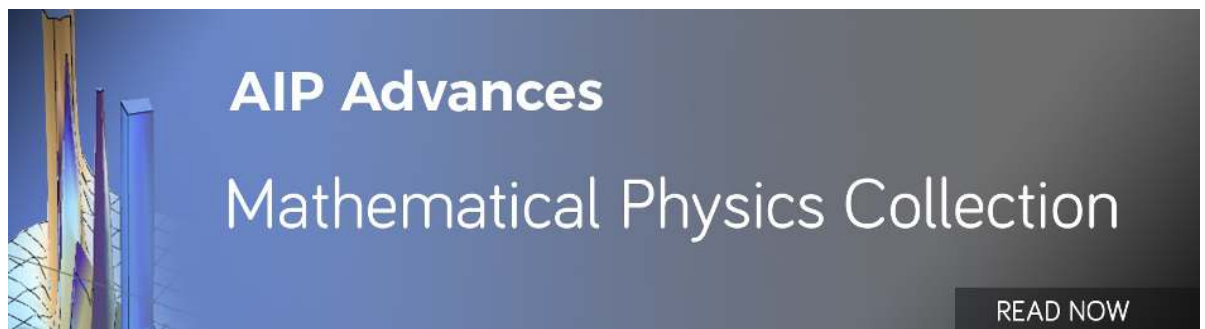
CrossMark

## ARTICLES YOU MAY BE INTERESTED IN

[Diaphragm shape effect on the performance of foil-based capacitive pressure sensors](#)  
AIP Advances **10**, 015009 (2020); <https://doi.org/10.1063/1.5128475>

[Multisensory graphene-skin for harsh-environment applications](#)  
Applied Physics Letters **117**, 074101 (2020); <https://doi.org/10.1063/5.0017769>

[Evaluation of ecological risk of heavy metals in watershed soils in the Daxia River Basin](#)  
AIP Advances **10**, 055109 (2020); <https://doi.org/10.1063/5.0004869>



# Metal coated polymer and paper-based cantilever design and analysis for acoustic pressure sensing

Cite as: AIP Advances 10, 055112 (2020); doi: 10.1063/5.0006544

Submitted: 5 March 2020 • Accepted: 18 April 2020 •

Published Online: 12 May 2020



R. B. Mishra,<sup>1,2</sup>  S. F. Shaikh,<sup>1</sup>  A. M. Hussain,<sup>2</sup>  and M. M. Hussain<sup>1,3,a)</sup> 

## AFFILIATIONS

<sup>1</sup>mmh Labs, Computer Electrical Mathematical Science, and Engineering Division (CEMSE), King Abdullah University of Science and Technology (KAUST), Thuwal 23955-6900, Saudi Arabia

<sup>2</sup>Center for VLSI and Embedded Systems Technology (CVEST), International Institute of Information Technology (IIIT), Hyderabad, Telangana 500032, India

<sup>3</sup>Electrical Engineering and Computer Sciences, University of California, Berkeley, California 94720, USA

<sup>a)</sup>Author to whom correspondence should be addressed: [muhammad.hussain@kaust.edu.sa](mailto:muhammad.hussain@kaust.edu.sa) and [mmhussain@berkeley.edu](mailto:mmhussain@berkeley.edu).  
Telephone: +966-2808-4450

## ABSTRACT

Cantilevers are one of the most utilized mechanical elements for acoustic sensing. In comparison to the edge clamped diaphragms of different shapes, a single edge clamped cantilever makes an acoustic sensor mechanically sensitive for detection of lower pressure. The aspect ratio of cantilevers is one of the most important parameters which affect sensitivity. Herein, we present a mathematical, finite element method and experimental analysis to determine the effect of the aspect ratio on the resonant frequency, response time, mechanical sensitivity, and capacitive sensitivity of a cantilever-based acoustic pressure sensor. Three cantilevers of different aspect ratios (0.67, 1, and 1.5) have been chosen for sound pressure application to detect capacitance change. The cantilever with the smallest aspect ratio (0.67) has the highest response time (206 ms), mechanical sensitivity, and capacitive sensitivity (22 fF), which reduce after increasing the aspect ratio. The resonant frequency of the cantilever was also analyzed by applying sweep in sound frequency. It was found to be minimum for the cantilever with the smallest aspect ratio (510 Hz) and increases with an increase in the aspect ratio. We have applied the garage fabrication process using low cost, recyclable, and easily available materials such as metal coated polymer sheets, mounting tapes and glass slides as alternative materials for expensive materials.

© 2020 Author(s). All article content, except where otherwise noted, is licensed under a Creative Commons Attribution (CC BY) license (<http://creativecommons.org/licenses/by/4.0/>). <https://doi.org/10.1063/5.0006544>

## I. INTRODUCTION

Paper and polymer-based materials have attracted huge attention due to several advantages like low cost, less weight, ready availability, flexibility, and no clean room requirement. These materials require simple instruments for crafting, cutting, folding, sculpting, and printing.<sup>1-4</sup> There have been several demonstrations where these materials and processes have been utilized for fabricating flexible devices like sensors, actuators, field-effect transistors, batteries, loudspeakers, memory devices, and e-skin, wearable, and environmental monitoring devices.<sup>1-8</sup>

Cantilevers are ubiquitous mechanically sensitive elements used in MEMS (micro-electro-mechanical-systems) for designing

pressure sensors,<sup>9</sup> accelerometers,<sup>10</sup> gyroscopes,<sup>11</sup> microphones,<sup>12</sup> flow sensors,<sup>13</sup> energy harvesters<sup>14</sup> and resonators in automobile,<sup>15</sup> robotics,<sup>16</sup> automobiles,<sup>17</sup> aerospace,<sup>18</sup> consumer electronics,<sup>12,13,19</sup> and chemical/biological industries.<sup>20</sup> Different principles of operation like capacitive sensing,<sup>9</sup> piezo-resistive,<sup>1</sup> or piezoelectric<sup>14</sup> have been demonstrated for pressure sensing from cantilevers. Among all these techniques, the MEMS capacitive sensing approach is the most pragmatic and holds an upper hand in the following parameters: low-cost, large fabrication area, low temperature hysteresis, high sensitivity, and high repeatability.<sup>21</sup> The key matrices for consideration in the capacitive pressure sensor design are Young's modulus of elasticity, Poisson's ratio, geometric parameters (shape, area, thickness, etc.) of mechanically sensitive elements, the dielectric medium,

and the separation gap between electrodes.<sup>22</sup> Traditionally, in the MEMS community, silicon-based materials are used to fabricate high-performance cantilevers although the processes are time consuming, expensive, and complex with multiple fabrication steps that necessitate a clean-room environment for largescale fabrication.<sup>1,21</sup> Emerging trends such as simplifying the fabrication processes, flexible electronics, and Internet-of-Things have been driving new design concepts toward cost effective and large-area electronic based cantilevers with different materials like paper, fibers, biopolymers, and metalized polymers.<sup>1,2,23,24</sup>

In coherence with paper/polymer-based electronics, cantilever based piezo-resistive devices have been reported using a common substrate material—paper and carbon ink as conducting elements.<sup>1</sup> Similarly, a weighing machine has been recently reported using a paper substrate material, forming a Wheatstone bridge circuit using conductive-silver ink responding to the change in resistance of the piezo-resistive material on application of pressure on the cantilever.<sup>1</sup> The cantilever shape, strain gauge, and piezo-resistive sensor have been designed using pencils on the paper substrate for resistance change, compression, and tensile strain measurement.<sup>25,26</sup> The properties of resistors change due to the use of different types of hardness and shades of pencils.<sup>26</sup> The low cost and simple and instant detection of different volatile organic compounds (methanol, ethanol, acetone, and tetrahydrofuran) through the naked eye using paper and swellable polymer-based cantilevers have been reported.<sup>8</sup> The polymer, adhered to the paper substrate, swells in the presence of volatile organic compounds due to which bending occurs in cantilevers. The bending angle has been monitored using a protractor which faces the cantilevers, and according to the bending angle, the volatile organic compound can also be detected.<sup>8</sup> Of all the different shapes (circle, ellipse, square, rectangle, and pentagon) of a diaphragm, the circularly shaped diaphragm has the highest sensitivity.<sup>27–29</sup> In these terms, the sensitivity of a cantilever is also dependent on the aspect ratio and thickness of cantilevers.<sup>7</sup> In this present work, we used aluminum sputtered polyamide sheets and double-sided post-it tapes to fabricate three different cantilevers of different aspect ratios while keeping the overlapping area between the parallel plates the same.

We present a parallel plate capacitive architecture-based pressure sensing cantilever consisting of two electrodes, one fixed as the bottom electrode whereas the other electrode as a mechanically sensitive floating electrode clamped to one of the edges. To analyze the different response parameters of cantilever capacitive pressure sensors (resonant frequency, sensitivity, response time, and stability of the system), the audible frequency range of sound has been applied as the pressure application source.

## II. GOVERNING EQUATIONS AND FEM-ANALYSIS

Pressure wave application on the cantilever causes a deflection in the cantilever due to which the capacitance varies. The base capacitance of the capacitive pressure sensor is given by

$$C = \epsilon \frac{A}{d}. \quad (1)$$

Here,  $\epsilon$ ,  $A$ , and  $d$  are the dielectric constant of the medium, overlapping area, and separation gap between the electrodes, respectively.

After pressure application on top of the cantilever, capacitance is given by

$$C = \iint_s \frac{\epsilon dA}{d - W}. \quad (2)$$

$S$  and  $W$  correspond to the surface area of the mechanically sensitive top electrode of the cantilever and cantilever deflection due to pressure wave application, respectively.

The deflection/bending properties of mechanically sensitive elements have remarkable influence on their static and dynamic behavior. The cantilever theory inhabits a special place in mechanics theory because a large number of mechanically sensitive elements follow a special geometric characteristic in which one dimension of those mechanical elements plays a very important role compared to the other two dimensions. For the small deflection theory or thin plate theory, the maximum deflection in a cantilever should be 1/5th its thickness. However, for the large deflection theory or thick plate theory, the maximum deflection in a cantilever should not be more than three times its thickness. Therefore, deflection in a large cantilever structure will behave as a dynamic non-linear model, which can be presented by the partial differential equation of Euler–Bernoulli's model:<sup>30</sup>

$$D \frac{\partial^4 W(x, t)}{\partial x^4} + m \frac{\partial^2 W(x, t)}{\partial t^2} + q(x, t) = 0; \forall x \in (0, L), t = 0, \quad (3)$$

where,  $D$ ,  $m$ , and  $q$  are the flexural rigidity of pressure sensitive cantilevers, mass per unit length of cantilevers and distributed load on cantilevers, respectively.

For this initial boundary value problem, the initial conditions are

$$W(x, t) = 0 \text{ and } \frac{\partial W(x, 0)}{\partial t} = 0; \forall x \in [0, L], \quad (4)$$

$$W(0, t) = 0, \quad \frac{\partial W(0, t)}{\partial t} = 0, \quad \frac{\partial^2 W(L, t)}{\partial t^2} = 0,$$

and

$$-D \frac{\partial^3 W(L, t)}{\partial t^3} = P(t), \forall t \geq 0, \quad (5)$$

where  $L$  is the effective length of a cantilever.

For non-stretchable cantilevers,

$$\int_0^{\bar{x}(t)} \sqrt{1 + \left( \frac{\partial W(x, t)}{\partial t} \right)^2} dx = L \text{ and } q(x, t) = 0; \forall t \geq 0. \quad (6)$$

The deflection in a cantilever due to pressure wave,  $P(t) = P_n \sin(\omega t)$ , can be given by

$$W(x, t) = \frac{P(t)}{2D\beta^3 [1 + (\cos \beta L)(\cosh \beta L)]} [\sin \beta(x - L) + \sinh \beta(L - x) - \cos \beta x \sinh \beta L + \sin \beta L \cosh \beta x + \sin \beta x \cosh \beta L - \cos \beta L \sinh \beta x], \quad (7)$$

where  $\beta = \sqrt[4]{m\omega^2/D}$  and  $\omega$  is the frequency of vibration.

In addition, the bending moment of the cantilever at the clamped edge can be given by

$$M(t) = D \left. \frac{\partial^2 w(x,t)}{\partial x^2} \right|_{x=0}. \quad (8)$$

Computer aided design (CAD) tools are commercially available to analyze the behavior of devices before fabricating them, which saves time and cost. These tools perform finite element method (FEM)-analysis when the devices are under certain physical, chemical, or biological conditions. Herein, the CoventorWare<sup>®</sup> software is used for analyzing three different cantilever-based capacitive pressure sensors of different aspect ratios, while the overlapping area between parallel plates is kept the same for all three designs, as shown Fig. 1(a). Different designs of the cantilever pressure sensor, D1, D2, and D3, of an aspect ratio of 27.27, 1.0, and 0.0366, respectively, have been chosen. The thickness of the mechanically sensitive diaphragm, overlapping area, and separation gap between both electrodes are 25.05  $\mu\text{m}$ , 0.15  $\text{cm}^2$ , and 250  $\mu\text{m}$ , respectively. D1 and D3 are identical with a difference in the edge, which is clamped, and D2 has a square shape of the same surface area as D1 and D3. The simulations for resonant frequency, mechanical sensitivity, and capacitive sensitivity have been performed for all three designs and found that there is a proper trend in all these parameters as the aspect ratio varies. The resonant frequency, which has the inverse square law relation with the length of the cantilever,<sup>12,31</sup> decreases as the aspect ratio of the cantilever decreases. The resonant frequency is minimum for D3, which has the smallest aspect ratio, as shown in Fig. 1(b). The mechanical as well as capacitive sensitivity increases

as the aspect ratio of the cantilever decreases, which is maximum for D3, as shown in Fig. 1(c).

### III. FABRICATION AND EXPERIMENTAL RESULTS

Experimental validation and analysis have been carried out in order to study the effect of varying aspect ratios on the sensitivity and resonant frequency of the cantilever. Consistent with our approach of the low-cost and simple garage fabrication technique, we use a commercially available thin aluminum coated polyimide (PI) sheet (Liren's LR-PI 100AM of 25  $\mu\text{m}$  polyimide coated with 200 nm aluminum) as our light-weight foil material. We followed a DIY approach in fabrication to simplify the processes and reduce the associated costs to make it widely acceptable and accessible. The detailed fabrication schematic is presented in Fig. 2. We start with a glass substrate ( $7.5 \times 5 \times 1 \text{ mm}^3$ ) as a carrier followed by adhering a thin PI sheet coated with Al on top of the substrate [Figs. 2(a) and 2(b)]. This Al coated PI sheet acts as the conductive electrode for the capacitive pressure sensor structure, while the insulating PI layer of the thin sheet provides mechanical support and strength to the conductive cantilever structure. Thus, the cantilever structure consists of two components: a conducting element (Al metal in this case) and a supporting thin PI layer. To form a parallel plate capacitive structure for the cantilever, we cut both the bottom and top electrodes from the same PI substrate attached to the glass carrier using a carbon dioxide ( $\text{CO}_2$ ) laser [Fig. 2(c)]. A Versa 2000  $\text{CO}_2$  laser cutter tool is used to make different patterns and shapes by scribing through the polymer film with high accuracy and selectivity

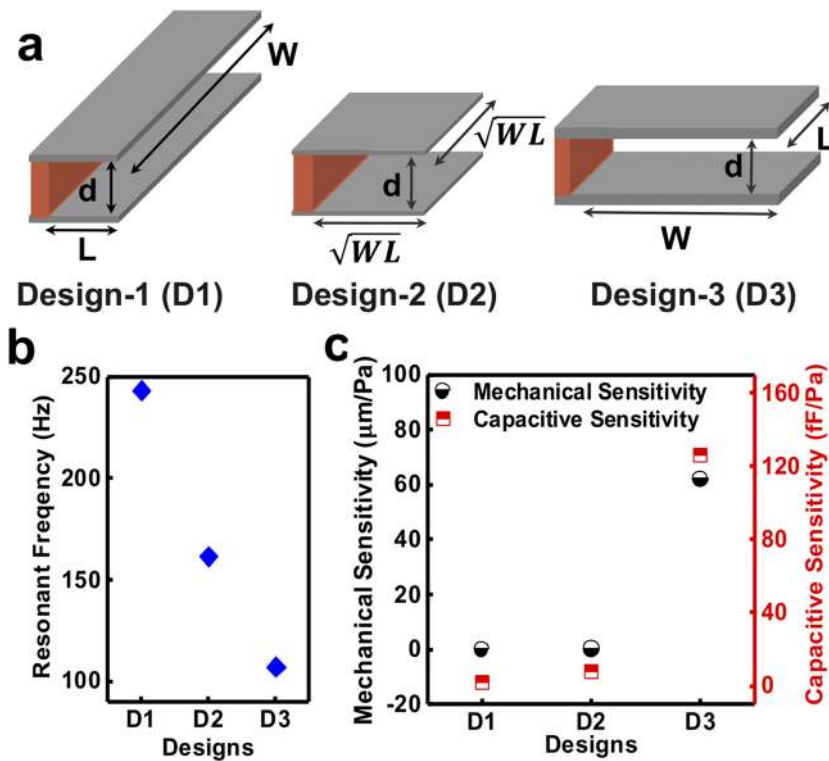


**FIG. 1.** (a) Schematic of three different designs of cantilever capacitive pressure sensors. The surface area of the diaphragm is the same for all three designs D1, D2, and D3, (b) the resonant frequency of all three designs using finite element simulation, and (c) mechanical and capacitive sensitivity of all three designs using finite element simulation at 1 Pa pressure.

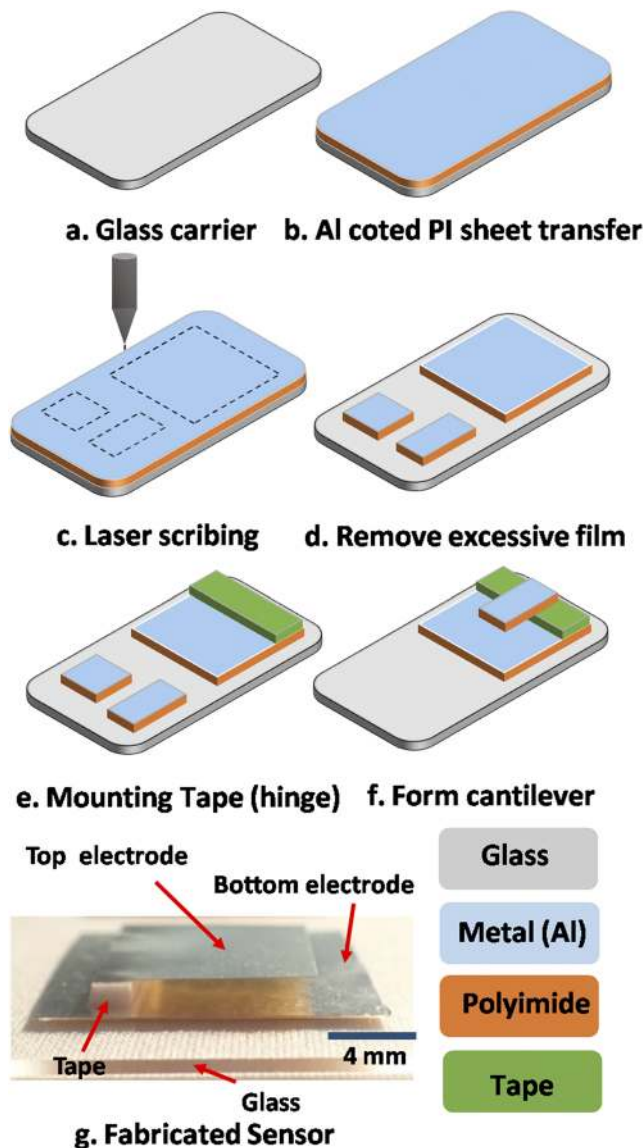


**FIG. 2.** [(a)–(f)] Schematic illustration of steps involved in fabricating cantilever capacitive pressure sensors in which (f) represents the final architecture of the sensor. (g) the digital photograph of the fabricated capacitive pressure sensor to show air as the dielectric layer (separation gap) which varies due to sound pressure application.

to pattern only the polymer film without affecting the carrier substrate. The parameters affecting the scribing process (power, speed, vertical separation between the laser and substrate, and frequency) were optimized (10% power, 20% speed, 2 mm separation, and a frequency of 1000 ppm). Because the cantilever structure primarily comprises a hanging beam clamped from one edge, as shown in Fig. 1, we have used a paper adhesive tape of a thickness of 1.5 mm, creating the clamp for the top electrode with the fixed bottom electrode having air as the dielectric layer for parallel plate capacitance,

shown in Figs. 2(d)–2(g). The thin PI sheet (foil) and the simple process of fabrication make it a low-cost process, compatible and readily adaptable for large area flexible sensor fabrication. Al coated PI films offer an enhanced linear range of elasticity<sup>27,29,32</sup> and flexural rigidity

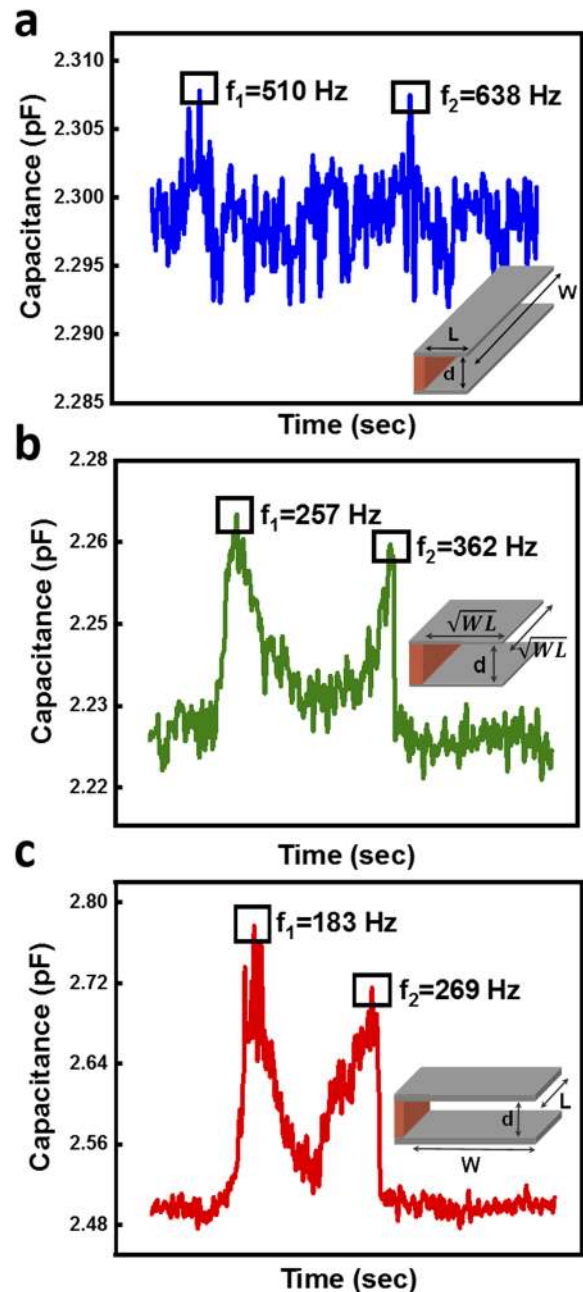


**FIG. 3.** Experimental investigation of the first and second mode of resonant frequencies ( $f_1$  and  $f_2$ ) after applying a sweep of 20 Hz to 20 kHz sound wave for three different cantilevers of the same aspect ratio of (a) 1.5, (b) 1.0, and (c) 0.67. All three cantilevers have the same overlapping area of 1.5 cm<sup>2</sup>. The first mode resonant frequency is known as the natural frequency, which is minimum for the cantilever with the smallest aspect ratio.

in the structure. Experimental validations have been performed on three aspect ratios of 0.67, 1, and 1.5 for the cantilever forming the top electrode of the capacitive pressure sensor with a constant area of  $1.5 \text{ cm}^2$ .

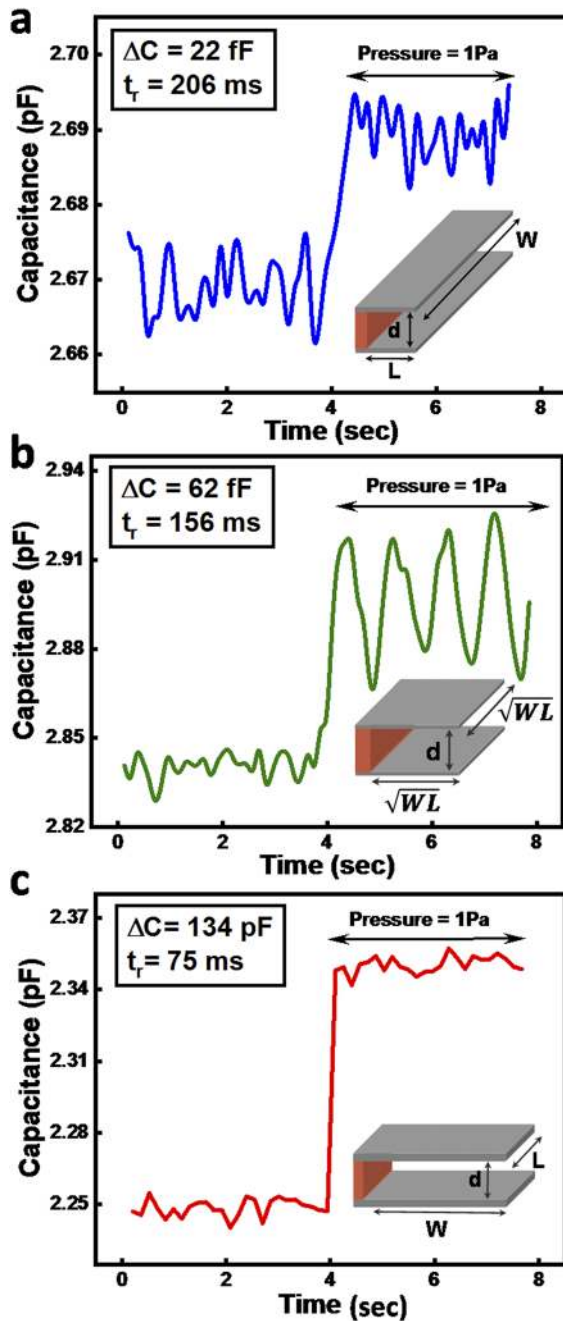


**FIG. 4.** (a) Experimental investigation of capacitance change and response time of all three different cantilever pressure sensors which have an aspect ratio of (a) 1.5, (b) 1.0, and (c) 0.67. A sound wave of 300 Hz frequency and 1 Pa pressure is applied. The cantilever pressure sensor with the smallest aspect ratio has the maximum sensitivity and minimum response time among all three sensors.

One of the widely accepted techniques for MEMS-based cantilevers, diaphragms, and microphone characterization is using a source of sound for applying pressure waves. However, cantilevers are more sensitive mechanical elements than diaphragms because cantilevers eliminate the clamped boundary conditions from three edges.<sup>33</sup> Finally, to obtain the resonant frequency and change in capacitance, a sound pressure of 94 dB intensity (corresponding to 1 Pa which is the same pressure applied on the sensors in FEM-simulations) is applied from the speaker (JBL Go portable wireless Bluetooth speaker). The speaker is kept 3 mm away from the sensors, and the sound is played from a smart phone. The capacitance change is monitored using a Keithley Semiconductor Characterization System (Model – 4200 SCS).

Using this sound pressure measuring setup, a sweep from 20 Hz to 20 kHz is applied on all the three designs obtaining resonant frequencies. The first and second mode of frequencies ( $f_1$  and  $f_2$ ) is obtained for all different cantilever pressure sensors, as shown in Figs. 3(a)–3(c). The aspect ratio for D3 is minimum; hence, the first and second mode of resonant frequencies is less, and the change in capacitance is maximum for the design with the smallest aspect ratio among all designs. It can be observed that the experimental result trends replicate the trends in all three designs from FEM-analysis. The occurrence of resonant frequency is the smallest in the design which has the smallest aspect ratio among all designs and increases as the aspect ratio of the cantilever increases, as shown in Figs. 3(a)–3(c). We observed that the design which has the smallest aspect ratio has the smallest gap between occurrence of the first and second mode resonant frequencies ( $f_2 - f_1$ ) among all designs due to which this design can be considered as the most stable system among all.

The capacitance change in all three designs at a frequency of 300 Hz is shown in Figs. 4(a)–4(c). 300 Hz frequency is chosen to apply sound pressure because it does not match (or is not close to) the resonant frequency of any design. The sound pressure deflects the diaphragm of the design which has the smallest aspect ratio among all and follows the same trend which has been shown in FEM-simulations for all designs. The response time ( $t_r$ ) of the sensor increases as the aspect ratio of the cantilever and the minimum rise time for the cantilever sensor of the smallest aspect ratio decrease, as mentioned in Figs. 4(a)–4(c).

#### IV. CONCLUSION

Cantilever and diaphragm-based pressure sensors have been an integral part of MEMS devices for a variety of applications like accelerometers, gyroscopes, flow-sensors, acoustic pressure sensors, and resonators. Recent trends in Internet-of-Things (IoT) based healthcare monitoring and connecting sensors with things have opened opportunities to look at new materials, processes, and simple manufacturing techniques to cope with the rapid pace of development.<sup>34,35</sup> Paper based sensing platforms have gained a significant thrust in this emerging area. Coherently, we have reported here a thin foil-based cantilever design and analysis for acoustic pressure sensors. A simple garage fabrication process, ready availability of raw ingredients, and a DIY approach provide great potential for the presented devices. The analysis of the effect of the geometrical design (aspect ratio) provides an insight into how geometrical parameters

play an important role for any sensor and what design shall be preferred based on the frequency spectrum and the envisioned application. After analyzing all three different designs of cantilevers whose aspect ratios are 0.67, 1, and 1.5, we conclude that the cantilever based capacitive pressure sensor which has the maximum aspect ratio gives rapid response, possesses maximum sensitivity, and is capable of responding to low frequency sound ( $f_2 - f_1 = 183$  Hz). The sensitivity (both mechanical and capacitive) and response time decrease as the aspect ratio decreases. The difference between occurrence of the first and second mode of resonant frequencies is undershot for the sensor with the maximum aspect ratio, which is advantageous for designing a stable system, which decreases as the aspect ratios decrease. Furthermore, in the future, more intense studies on applications relevant to human health monitoring, flow-sensing, and environmental monitoring can be explored by making design modifications and considering various material choices.

## ACKNOWLEDGMENTS

This publication is based on the work supported by the King Abdullah University of Science and Technology (KAUST) Office of Sponsored Research (OSR) under KAUST–KFUPM Special Initiative Award No. OSR-2016-KKI-2880.

## DATA AVAILABILITY

The data that support the findings of this study are available from the corresponding author upon reasonable request.

## REFERENCES

- J. Fu, T. Zhu, Y. Liang, Z. Liu, R. Wang, X. Zhang, and H. X. Wang, *Sci. Rep.* **9**(1), 4699 (2019).
- H. Seidel and L. Csepregi, *Sens. Actuators* **6**(2), 81–92 (1984).
- K. Maenaka, T. Fujita, Y. Konishi, and M. Maeda, *Sens. Actuators, A* **54**(1-3), 568–573 (1996).
- S. Dass and R. Jha, *Sci. Rep.* **8**(1), 12701 (2018).
- F. Hu, Y. Qian, Z. Li, J. Niu, K. Nie, X. Xiong, W. Zhang, and Z. Peng, *J. Opt.* **15**(5), 055101 (2013).
- H. Liu, J. Zhong, C. Lee, S.-W. Lee, and L. Lin, *Appl. Phys. Rev.* **5**(4), 041306 (2018).
- M. Liao, M. Toda, L. Sang, S. Hishita, S. Tanaka, and Y. Koide, *Appl. Phys. Lett.* **105**(25), 251904 (2014).
- K. Noda, Y. Hashimoto, Y. Tanaka, and I. Shimoyama, in *IEEE International Solid-State Sensors, Actuators and Microsystems Conference* (IEEE, 2009), pp. 2176–2181.
- K. H. Kim, J. S. Ko, Y. H. Cho, K. Lee, B. M. Kwak, and K. Park, *Sens. Actuators, A* **50**(1-2), 121–126 (1995).
- S. Janson, H. Helvajian, and K. Breuer, in *30th Fluid Dynamics Conference* (American Institute of Aeronautics and Astronautics (AIAA), 1999), p. 3802.
- M. Possas-Abreu, L. Rousseau, F. Ghassemi, G. Lissorgues, M. Habchi, E. Scorsone, K. Cal, and K. Persaud, in *ISOCS/IEEE International Symposium on Olfaction and Electronic Nose (ISOEN)* (IEEE, 2017), pp. 1–3.
- M. Nordström, S. Keller, M. Lillemose, A. Johansson, S. Dohn, D. Haefliger, G. Blagoi, M. Havsteen-Jakobsen, and A. Boisen, *Sensors* **8**(3), 1595–1612 (2008).
- X. Liu, M. Mwangi, X. Li, M. O'Brien, and G. M. Whitesides, *Lab Chip* **11**(13), 2189–2196 (2011).
- J. Li, R. Bao, J. Tao, Y. Peng, and C. Pan, *J. Mater. Chem. C* **6**(44), 11878–11892 (2018).
- N. Minh-Dung, H. Takahashi, T. Uchiyama, K. Matsumoto, and I. Shimoyama, *Appl. Phys. Lett.* **103**(14), 143505 (2013).
- J. M. Nassar, M. D. Cordero, A. T. Kutbee, M. A. Karimi, G. A. T. Sevilla, A. M. Hussain, and M. M. Hussain, *Adv. Mater. Technol.* **1**(1), 1600004 (2016).
- H. Macicior, E. Ochoteco, G. Cabañero, H. Grande, O. Schwarzhaupt, M. Lehmann, and A. Büter, *Procedia Eng.* **5**, 641–644 (2010).
- M. Chason, D. R. Gamota, P. W. Brazis, K. Kalyanasundaram, J. Zhang, K. K. Lian, and R. Crosswell, *MRS Bull.* **31**(6), 471–475 (2006).
- G. Wang, T. Cheng, Y. Do, H. Yang, Y. Tao, J. Gu, B. An, and L. Yao, in *Proceedings of the 2018 CHI Conference on Human Factors in Computing Systems* (Association for Computing Machinery (ACM), 2018), p. 569.
- H. Oh, T. D. Ta, R. Suzuki, M. D. Gross, Y. Kawahara, and L. Yao, in *CHI* (Association for Computing Machinery (ACM), 2018), p. 441.
- R. Martins, A. Nathan, R. Barros, L. Pereira, P. Barquinha, N. Correia, R. Costa, A. Ahnood, I. Ferreira, and E. Fortunato, *Adv. Mater.* **23**(39), 4491–4496 (2011).
- E. Fortunato, N. Correia, P. Barquinha, L. Pereira, G. Goncalves, and R. Martins, *IEEE Electron Device Lett.* **29**(9), 988–990 (2008).
- R. Martins, I. Ferreira, and E. Fortunato, *Phys. Status Solidi RRL* **5**(9), 332–335 (2011).
- A. Fraiwan, H. Lee, and S. Choi, *Talanta* **158**, 57–62 (2016).
- C. W. Lin, Z. Zhao, J. Kim, and J. Huang, *Sci. Rep.* **4**, 3812 (2014).
- T.-K. Kang, *Appl. Phys. Lett.* **104**(7), 073117 (2014).
- S. M. Khan, R. B. Mishra, N. Qaiser, A. M. Hussain, and M. M. Hussain, *AIP Adv.* **10**(1), 015009 (2020).
- T. Wang, X. Mu, A. B. Randles, Y. Gu, and C. Lee, *Appl. Phys. Lett.* **107**(12), 123501 (2015).
- S. M. Khan, N. Qaiser, S. F. Shaikh, and M. M. Hussain, *IEEE Trans. Electron Devices* **67**(1), 249–257 (2020).
- Y. A. Antipov, *Proc. R. Soc. A* **470**(2170), 20140064 (2014).
- J. W. Yi, W. Y. Shih, and W.-H. Shih, *J. Appl. Phys.* **91**(3), 1680–1686 (2002).
- G. T. Mearini and R. W. Hoffman, *J. Electron. Mater.* **22**(6), 623–629 (1993).
- H. Takahashi, N. M. Dung, K. Matsumoto, and I. Shimoyama, *J. Micromech. Microeng.* **22**(5), 055015 (2012).
- A. M. Hussain and M. M. Hussain, *Adv. Mater.* **28**(22), 4219–4249 (2016).
- M. M. Hussain, J. M. Nassar, S. M. Khan, S. F. Saikh, G. A. T. Sevilla, A. T. Kutbee, R. R. Bahabry, W. Babatatin, A. S. Muslem, M. Nour, I. Wicaksono, and K. Mishra, in *IEEE Sensors* (IEEE, 2017), pp. 1–2.